NEK7 is required for G1 progression and procentriole formation

Akshari Gupta[a,b], Yuki Tsuchiya[a,b], Midori Ohta[a], Gen Shiratsuchi[a], and Daiju Kitagawa[a,b,*]
[a]Division of Centrosome Biology, Department of Molecular Genetics, National Institute of Genetics, Mishima, Shizuoka 411-8540, Japan; [b]Department of Genetics, School of Life Science, Graduate University for Advanced Studies (SOKENDAI), Mishima, Shizuoka 411-8540, Japan

ABSTRACT **The decision to commit to the cell cycle is made during G1 through the concerted action of various cyclin–CDK complexes. Not only DNA replication, but also centriole duplication is initiated as cells enter the S-phase. The NIMA-related kinase NEK7 is one of many factors required for proper centriole duplication, as well as for timely cell cycle progression. However, its specific roles in these events are poorly understood. In this study, we find that depletion of NEK7 inhibits progression through the G1 phase in human U2OS cells via down-regulation of various cyclins and CDKs and also inhibits the earliest stages of procentriole formation. Depletion of NEK7 also induces formation of primary cilia in human RPE1 cells, suggesting that NEK7 acts at least before the restriction point during G1. G1-arrested cells in the absence of NEK7 exhibit abnormal accumulation of the APC/C cofactor Cdh1 at the vicinity of centrioles. Furthermore, the ubiquitin ligase APC/C^{Cdh1} continuously degrades the centriolar protein STIL in these cells, thus inhibiting centriole assembly. Collectively our results demonstrate that NEK7 is involved in the timely regulation of G1 progression, S-phase entry, and procentriole formation.**

Monitoring Editor
Manuel Théry
CEA, Hopital Saint Louis

Received: Sep 12, 2016
Revised: Apr 27, 2017
Accepted: May 18, 2017

INTRODUCTION

After mitotic exit, mammalian cells must make several important decisions based on extracellular and intracellular conditions during the G1 phase, which determine whether or not they will commit to enter a new cell cycle. Progression through G1 and transition into the S-phase are largely under the control of G1 cyclins and cyclin-dependent kinases (CDKs), which interact with and phosphorylate many different proteins to initiate DNA replication. During early G1, extracellular growth factor–mediated signaling pathways are necessary for passage through the restriction point, in the absence of which, cells exit the cell cycle into G0 and become quiescent (Foster *et al.*, 2010). Passage through the restriction point is largely contingent on the activity levels of cyclin D–CDK4/6 complexes (Narasimha *et al.*, 2014), which activate cyclin E–CDK2 complexes and the E2F family of transcription factors, initiating the expression of numerous genes required for S-phase entry (Foster *et al.*, 2010; Bertoli *et al.*, 2013). These surges in transcription toward late G1 create several positive feedback loops that result in the commitment of cells to enter the cell cycle.

Initiation of DNA replication is the major goal and consequence of S-phase entry. However, another important event that is initiated in most metazoan cells at the G1/S transition is centriole duplication, in which daughter centrioles start to assemble at the proximal ends of two existing mother centrioles toward later G1 and continue to elongate through the S-phase. Centrioles must be duplicated exactly once per cell cycle, as aberrations in centriole number can result in chromosome segregation defects. To ensure centriole number control, the various stages of centriole duplication and the centrosome cycle are under strict control. In particular, several core structural components required for the earliest stages of the assembly of daughter centrioles, also known as procentrioles, are tightly regulated. In humans, Polo-like kinase 4 (PLK4) is the primary initiator of procentriole assembly, and its expression and activity are

This article was published online ahead of print in MBoC in Press (http://www.molbiolcell.org/cgi/doi/10.1091/mbc.E16-09-0643) on May 24, 2017.
The authors declare that they have no competing financial interests.
A.G. and D.K. designed the study and the experiments; M.O. and G.S. performed preliminary experiments; A.G. performed the experiments reported here; Y.T. assisted in experimental setup; A.G. and D.K. analyzed data; A.G. and D.K. wrote the manuscript.
*Address correspondence to: Daiju Kitagawa (dkitagaw@nig.ac.jp).
Abbreviations used: APC/C, anaphase-promoting complex/cyclosome; CDK, cyclin-dependent kinase; NEK, NIMA-related kinase; PCM, pericentriolar material; PLK, Polo-like kinase.

heavily regulated by a number of factors, such as cell cycle–dependent transcription (Fischer *et al.*, 2014), cyclin–CDK complexes (Habedanck *et al.*, 2005; Zitouni *et al.*, 2016), autophosphorylation (Guderian *et al.*, 2010; Klebba *et al.*, 2015a,b), degradation (Cunha-Ferreira *et al.*, 2009, 2013; Klebba *et al.*, 2013), and binding to the procentriole component STIL (Ohta *et al.*, 2014; Kratz *et al.*, 2015; Moyer *et al.*, 2015). Binding of PLK4 to STIL promotes the recruitment of SAS-6 to the procentriole, which is the major structural component of the centriolar cartwheel (Dzhindzhev *et al.*, 2014; Ohta *et al.*, 2014). Because of the time-sensitive nature of centriole duplication, the expression levels of PLK4, STIL, and SAS-6 must be kept strictly under check as overexpression of either of these proteins is sufficient to induce centriole amplification (Kleylein-Sohn *et al.*, 2007; Strnad *et al.*, 2007; Vulprecht *et al.*, 2007; Tang *et al.*, 2011; Arquint *et al.*, 2012). Indeed, both STIL and SAS-6 are present at almost negligible levels during early G1 phase, and their expression and centriolar localization increase toward late G1 for procentriole assembly (Strnad *et al.*, 2007; Arquint *et al.*, 2012), and at least the promoter of the STIL gene has been shown to be under the control of E2F transcription factors (Erez *et al.*, 2008). After centriole duplication, STIL and SAS-6 protein levels remain relatively high for the remainder of the cell cycle until mitotic exit, upon which they are both targeted for degradation by the anaphase-promoting complex/cyclosome (APC/C) bound to its cofactor Cdh1 (Strnad *et al.*, 2007; Arquint and Nigg, 2014). The APC/C is a multisubunit E3 ubiquitin ligase important for promoting G1 progression (Qiao *et al.*, 2014) and plays a complex role in synchronizing the centrosome cycle with the cell cycle. Although specific details of APC/C functions at the centrosomes are unknown, it can mediate localized proteasomal degradation of several centrosomal and cell cycle–related proteins at the centrosomes (Fisk, 2012). Thus the events leading up to S-phase entry and centriole duplication are meticulously regulated in a spatiotemporal manner, and disruption of these events often leads to a prolonged G1 arrest or cell cycle exit.

Great progress has been made in the identification of the many molecules that regulate G1 progression and centriole duplication; however, the mechanisms by which they play discernible roles in the cell cycle are poorly understood. One such molecule is the kinase NEK7 from the NIMA-related kinase (NEK) family. Some of the earliest studies on NEK7 found it to be crucial for mitotic spindle organization and cytokinesis (Yissachar *et al.*, 2006; Kim *et al.*, 2007; Regan and Fry, 2009; Salem *et al.*, 2010) and also reported that NEK7 is required for centriole duplication and centrosome cycle progression (Yissachar *et al.*, 2006; Kim *et al.*, 2007, 2011). Atypical overexpression of NEK7 has been implicated in various cancers (Wang *et al.*, 2013; Saloura *et al.*, 2015; Zhou *et al.*, 2016) and possibly can induce proliferation of otherwise resting cells (Kooi *et al.*, 2016), suggesting that NEK7 has oncogenic potential. Similarly, down-regulation of NEK7 can lead to a delay in S-phase entry (Kim *et al.*, 2011; Saloura *et al.*, 2015) and early mortality during murine embryogenesis (Salem *et al.*, 2010). Although these studies indicate that NEK7 may play a crucial role in the progression of the cell cycle and particularly during G1, how exactly NEK7 may contribute to cell cycle regulation has been unclear. Thus we decided to conduct a detailed investigation on the effect of NEK7 depletion on cell cycle progression and centriole duplication. Here we report that the depletion of NEK7 is sufficient to arrest cells in G1 and also causes centrosomal accumulation of the APC/C cofactor Cdh1, which negatively regulates centriole duplication.

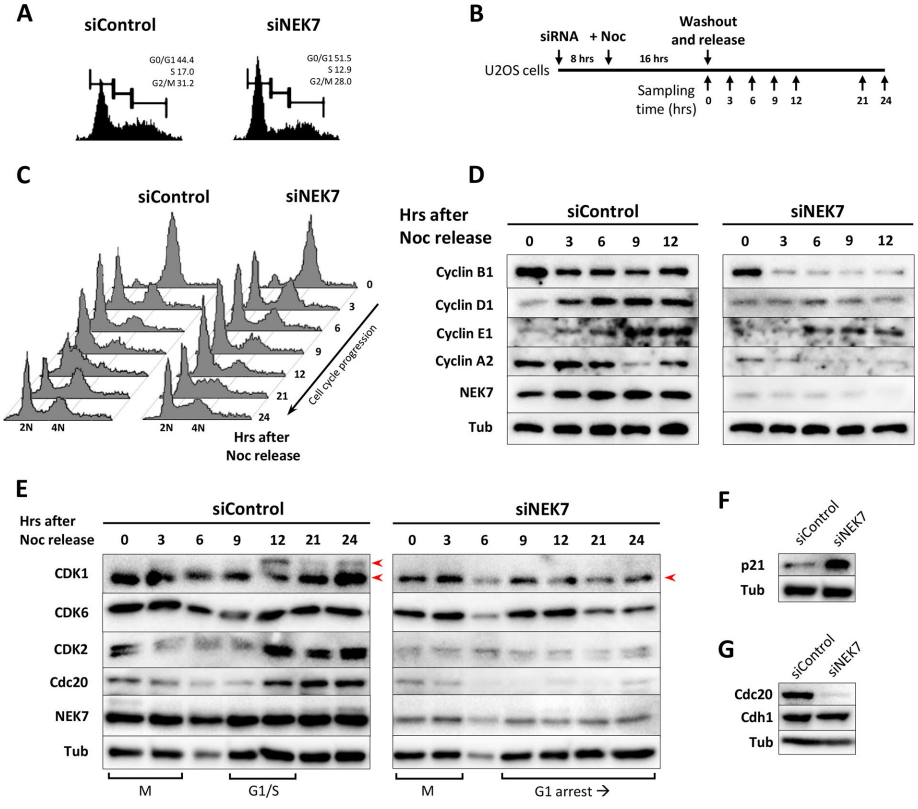

FIGURE 1: Depletion of NEK7 causes a G1-phase arrest. (A) Asynchronous U2OS cells were transfected with control or NEK7 siRNAs for 48 h, and the cells were analyzed for their DNA content profiles. (B) Schematic of the experimental conditions in C–E. U2OS cells were transfected with control or NEK7 siRNAs for 8 h and then synchronized at early mitosis with 100 ng/ml nocodazole (Noc) for 16 h. The cells were then released into fresh medium and collected at the indicated time points. (C) The DNA content profiles for individual time points. (D, E) Total cell lysates were analyzed by immunoblotting using antibodies against the indicated proteins at least twice. All samples treated with control and NEK7 siRNAs were blotted on the same membrane; they have been separated for clarity. The cells used in E are the same as those in C. Red arrowheads indicate band-shifted proteins. (F, G) U2OS cells were treated as in A, and total cell lysates were analyzed by immunoblotting against the indicated antibodies.

RESULTS

NEK7 depletion causes a G1 arrest

Depletion of NEK7 has been shown to have an effect on cell cycle progression, causing a range of phenotypes, including prometaphase arrest with spindle assembly defects (Yissachar *et al.*, 2006; Kim *et al.*, 2007; Regan and Fry, 2009), delays in the cell cycle, and inhibition of cell proliferation (Kim *et al.*, 2011; Saloura *et al.*, 2015). Our initial experiments indicated that treatment with small interfering RNA (siRNA) against NEK7 in asynchronous U2OS cell cultures caused a slight increase in the G0/G1 cell population compared with cells treated with control siRNA (Figure 1A). To confirm whether these cells indeed represent a cell cycle arrest, we arrested U2OS cells that were treated with

control or NEK7 siRNAs at early mitosis using nocodazole and then released them into fresh medium (Figure 1B). This enabled us to examine whether these cells were capable of exiting mitosis and continuing with the next cell cycle. We found that although most NEK7-depleted cells exited mitosis, most were unable to exit G1 phase and initiate DNA replication (Figure 1C and Supplemental Figure S2A).

To further characterize these cell cycle delays in cells lacking NEK7, we analyzed the expression levels of various cyclins and CDKs in total cell lysates collected at different points after nocodazole release (Figure 1, D and E). Expression levels of the mitotic cyclin B1 decreased in cells treated with NEK7 siRNA compared with control cells upon mitotic exit (Figure 1D). CDK1, which forms a complex with cyclin B1, undergoes inhibitory phosphorylations during interphase to prevent premature mitotic entry (Ayeni and Campbell, 2014), as can be seen by an upshifted band at the 12-h time point in control cells (Figure 1E, red arrows). In contrast, CDK1 did not appear to undergo phosphorylation in NEK7-depleted samples, presumably reflecting the cell cycle delay in G1. Cyclin D1, which forms complexes with CDK4 and CDK6 in early G1, functions in passage through the restriction point, and low levels of cyclin D1 were associated with G1 arrest in previous studies (Masamha and Benbrook, 2009; Foster *et al.*, 2010). Of interest, expression of cyclin D1 was drastically reduced during G1 in NEK7-depleted cells, even though CDK6 levels did not appear to be significantly affected (Figure 1, D and E), suggesting that the cells may not be able to pass the restriction point. In late G1, cyclin E1 forms a complex with CDK2 to mediate the G1/S transition by increasing E2F-mediated transcription (Bertoli *et al.*, 2013). Remarkably, even though cyclin E1 levels remained unaltered (Figure 1D), CDK2 levels were severely down-regulated in NEK7-depleted cells (Figure 1E). Cyclin A2, which gradually replaces cyclin E1 in the complex with CDK2 during S-phase progression, also exhibited very low expression levels in NEK7-depleted cells (Figure 1D). The APC/C cofactor Cdc20, which is expressed from early S-phase to late mitosis, was also significantly down-regulated upon NEK7 depletion (Figure 1E). Taken together, these results strongly suggest that NEK7 is required for cell cycle progression during early G1 phase.

To further confirm that NEK7 depletion induces a G1 arrest, we looked at p21 levels in U2OS cells that were treated with control and NEK7 siRNAs for 48 h. It is known that high levels of p21 can inhibit S-phase entry through the direct inhibition of CDK2 activity as well as by binding proliferating cell nuclear antigen (PCNA) to inhibit DNA synthesis (Abbas and Dutta, 2009). In accordance with our results, we found significantly elevated levels of p21 in NEK7-depleted cells (Figure 1F and Supplemental Figures S1A and S3, A and B). Furthermore, upon expression of an RNA interference–resistant mutant of wild-type NEK7 (RR), cells exhibiting high cytoplasmic NEK7 RR levels were found to have drastically reduced p21 levels (Supplemental Figure S3, C and D). Thus we conclude that depletion of NEK7 is sufficient to arrest or delay cells at the G1 stage of the cell cycle.

Considering that the expression levels of several important cell cycle proteins required for proper G1 progression are affected upon depletion of NEK7 (Figure 1, D–F), we next investigated whether cells that are already in S-phase can complete DNA replication and undergo mitosis normally in the absence of NEK7. To overcome the G1 arrest that was induced upon prolonged NEK7 depletion, we treated U2OS cells with either control or NEK7 siRNAs for 8 h and then arrested these cells at the G1/S transition or in S-phase by adding thymidine to the medium for 16 h, followed by subsequent release into fresh medium and sample collection (Figure 2A). The short duration of siRNA treatment ensured that the majority of cells had not yet been arrested in G1 (Figure 2, A and B, and Supplemental Figure S2B), allowing us to characterize the progression through the rest of the cell cycle in NEK7-depleted cells. The DNA content profiles of cells treated with siNEK7 indicated that most of these cells completed DNA replication, albeit with a slight delay, and some of these cells completed mitosis as well (Figure 2B and Supplemental Figure S2B). As seen previously (Figure 1D), the expression levels of cyclin D1 were strongly decreased in NEK7-depleted cells, even though they remained elevated during S-phase progression in control cells (Figure 2C). Reduced levels of the late G1 cyclin E1 in both control and NEK7 siRNA–treated cells toward the 12-h time point confirmed that the cells were not arrested in G1 in this condition and could progress through S-phase (Grim *et al.*, 2008). However, S-phase cyclin A2 and CDK2 levels were still significantly low in these cells compared with control cells (Figure 2, C and D). Cdc20 protein levels were also drastically decreased in NEK7-depleted cells despite progression of the cell cycle (Figure 2D). Depletion of cyclin A2 causes delays in the G2/M transition (De Boer *et al.*, 2008; Gong and Ferrell, 2010; Barr *et al.*, 2016), and Cdc20 plays a crucial role in the spindle assembly checkpoint for

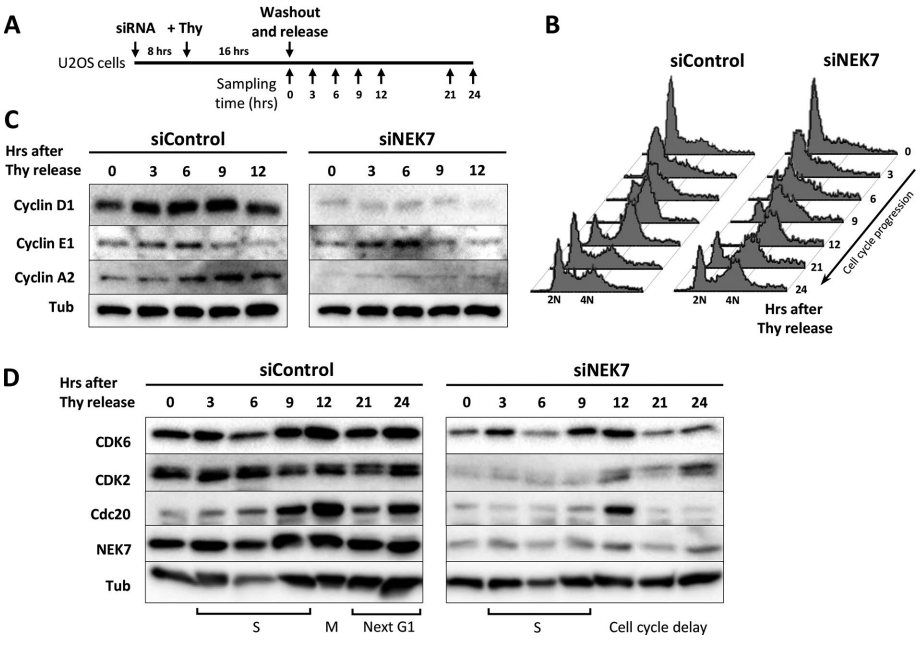

FIGURE 2: NEK7-depleted cells show cell cycle progression defects other than a G1-phase arrest. (A) Schematic of the experimental conditions in B–D. U2OS cells were transfected with control or NEK7 siRNAs for 8 h and then synchronized at S-phase with 2 mM thymidine (Thy) for 16 h. The cells were then released into fresh medium and collected at the indicated time points. (B) The DNA content profiles for individual time points. (C, D) Total cell lysates were analyzed by immunoblotting using antibodies against the indicated proteins at least twice. All samples treated with control and NEK7 siRNAs were blotted on the same membrane; they have been separated for clarity. The cells used in D are the same as those in B.

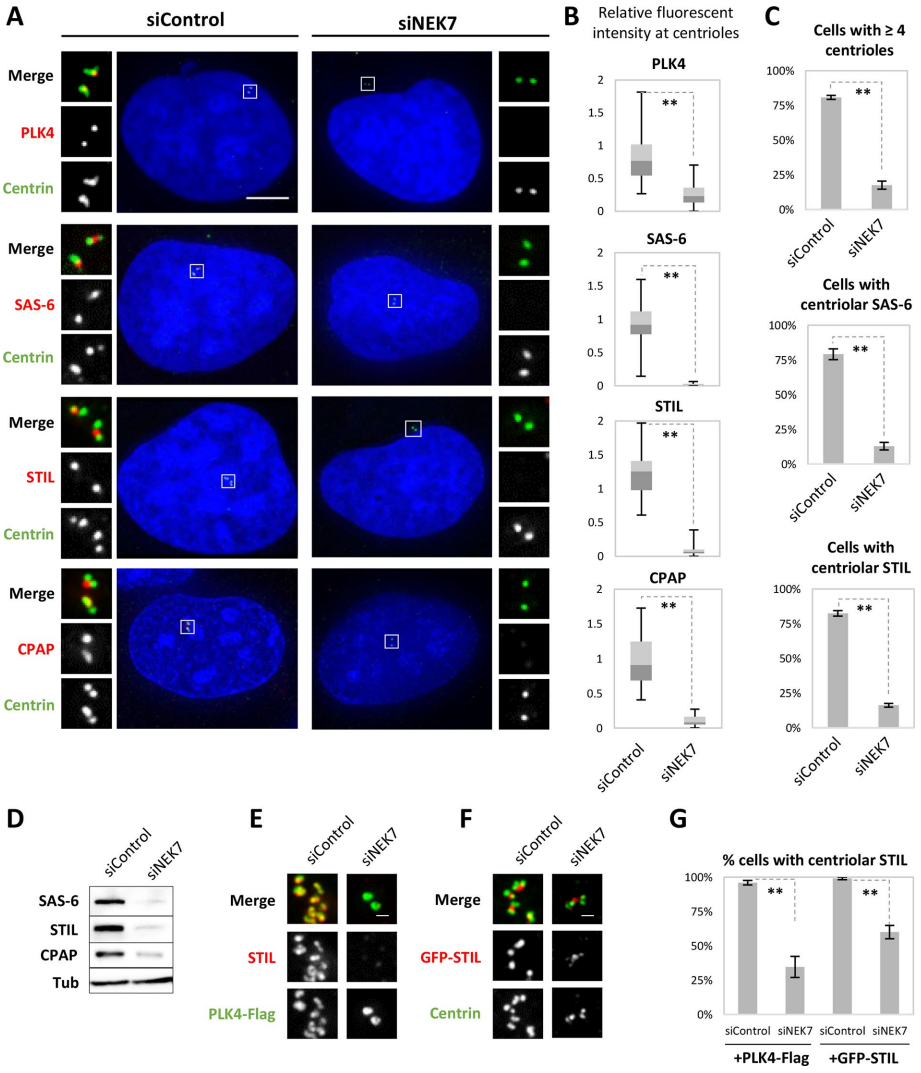

FIGURE 3: NEK7 is required for procentriole formation. (A) Asynchronous U2OS cells were transfected with control or NEK7 siRNAs for 48 h, and the cells were fixed and immunostained using the indicated antibodies. DNA is shown in blue. Insets are magnified views of the centrosomes. Scale bar, 5 μm. (B) Fluorescence intensities of the indicated proteins at the centrioles quantified on an arbitrary scale. (C) Percentage of interphase cells with the indicated centriolar markers. More than 50 cells were counted in each experimental group. (D) U2OS cells were treated as in A, and total cell lysates were analyzed by immunoblotting against the indicated proteins. (E) U2OS cells were transfected with control or NEK7 siRNAs. After 24 h, they were transfected with PLK4-ΔPEST-Flag for 24 h and then fixed. (F) GFP-STIL U2OS cells were transfected with control or NEK7 siRNAs, simultaneously induced for overexpression of GFP-STIL, and fixed after 48 h. Cells in E and F were immunostained with antibodies specific to STIL or GFP (red) and Flag or Centrin (green). Scale bar, 500 nm. (G) Population distributions of interphase cells containing centriolar STIL foci. More than 50 cells expressing high and comparable fluorescence intensities of PLK4-ΔPEST-Flag/GFP-STIL were counted in each experimental group. All histogram values are mean percentages ± SD from three independent experiments. $^{**}p < 0.01$; one-tailed *t* test.

chromosome segregation (Musacchio and Salmon, 2007); hence low levels of cyclin A2 and Cdc20 can largely account for the significant mitotic delays seen in these NEK7-depleted cells (Figure 2B), as well as previously reported mitotic defects (Yissachar *et al.*, 2006; Kim *et al.*, 2007; Regan and Fry, 2009; Salem *et al.*, 2010). Collectively our results suggest that the various defects in cell cycle progression observed upon depletion of NEK7 can be mostly explained by anomalous down-regulation in the expression levels of several critical cell cycle proteins.

NEK7 is required for procentriole formation

Our results so far demonstrate that NEK7 plays an important role in G1-phase progression, and may be required for proper progression through the rest of the cell cycle as well. Because the centrosome cycle is tightly linked to cell cycle progression, and procentriole formation is initiated at the G1/S transition, we speculated that NEK7 might perturb the earliest stages of centriole duplication as well. The knockdown of NEK7 has been reported to inhibit centriole duplication, as well as to reduce the total amount of pericentriolar material (PCM) that surrounds the centrioles and is required for the nucleation of spindle microtubules (Kim *et al.*, 2011). In addition, the PCM has been suggested to provide a suitable environment for centriole assembly by recruiting essential proteins (Strnad and Gönczy, 2008), which was suggested to be the reason for the inhibition of centriole duplication in the absence of NEK7 (Kim *et al.*, 2011). However, centriole duplication is a multistage process, and both centriole duplication and PCM assembly are heavily dependent on the activities of various CDKs (Harrison *et al.*, 2011; Wang *et al.*, 2014). Considering our results that NEK7 is required for the G1/S transition and affects the expression of various cyclin–CDK complexes, we speculated that some of the components required for the early stages of procentriole formation may also be affected upon NEK7 depletion. To address this, we checked various proteins involved in the procentriole assembly pathway, using the distal centriolar protein centrin as a marker for the number of centrioles (Figure 3, A–C). In accordance with previous studies (Kim *et al.*, 2011), most of the NEK7-depleted cells could not complete centriole duplication (Figure 3, A and C; ~18% of siNEK7 cells had ≥4 centrioles compared with ~81% in control cells), confirming that NEK7 is essential for centriole duplication. We found that CEP192 and CEP152, which are the earliest scaffold proteins to promote procentriole assembly (Sonnen *et al.*, 2013), were not affected upon NEK7 depletion (see later discussion of Figure 7, A, C, and E). However, the kinase PLK4, which depends on CEP192 and CEP152 for centriolar recruitment, was absent from the centrosomes (Figure 3, A and B). Similarly, STIL and SAS-6, which are essential for centriolar cartwheel formation, as well as centrosomal P4.1-associated protein (CPAP), which is required for centriole elongation (Schmidt *et al.*, 2009; Tang *et al.*, 2009), were also absent from the centrosomes upon NEK7 depletion (Figure 3, A–C). Surprisingly, we found that the levels of STIL, SAS-6, and CPAP were low not only at the centrosomes but also

in total cell lysates upon NEK7 depletion, as determined by immunoblotting analyses (Figure 3D and Supplemental Figure S1A). STIL, SAS-6, and CPAP are cell cycle–regulated proteins, and their expression levels increase during late G1 (Strnad *et al.*, 2007; Tang *et al.*, 2009; Arquint *et al.*, 2012). Thus it is likely that the reduction in their cytoplasmic and centrosomal levels that was observed upon NEK7 depletion is a consequence of the G1 arrest.

Overexpression of PLK4, STIL, or SAS-6 causes amplification of centrioles independently of cell cycle–mediated regulation on the centrosomes (Habedanck *et al.*, 2005; Leidel *et al.*, 2005; Arquint *et al.*, 2012). Hence we speculated about whether overexpression of these proteins might be sufficient to rescue centriole duplication in NEK7-depleted cells. Whereas overexpression of PLK4 and STIL induced centriole overduplication in control cells as expected, in cells pretreated with NEK7 siRNA, both centriole numbers and the numbers of PLK4/STIL foci were reduced (Figure 3, E–G). Of interest, in cells depleted of NEK7 and overexpressing PLK4, PLK4 formed ring-like foci (Figure 3E), which is reminiscent of the phenotype associated with the depletion of STIL (Ohta *et al.*, 2014). This result suggests that, despite high PLK4 levels, centriole amplification was inhibited by the absence of STIL and possibly other procentriolar proteins. Furthermore, given that overexpression of STIL did not rescue the expression levels of STIL at centrioles in NEK7-depleted cells (Figure 3, F and G), NEK7 may have an additional role in the maintenance of STIL at centrioles. Taken together, these results suggest that inhibition of procentriole formation upon NEK7 depletion is due to low cytoplasmic expression levels of several important procentriole proteins, possibly caused by the G1 arrest.

Depletion of NEK7 induces ciliogenesis

To assess the timing of the G1 arrest induced by the absence of NEK7, we decided to look at another centriole-associated phenotype that occurs as cells enter the G0/G1 phase. Several types of cells, such as RPE1 cells, frequently undergo ciliogenesis upon serum starvation, a method commonly used to arrest cells at the restriction point. During ciliogenesis, one of the unduplicated centrioles docks at the cell membrane for the formation of the primary cilium. Because several NEKs have been implicated in the regulation of ciliogenesis (Fry *et al.*, 2012), we tested whether NEK7-depleted cells also undergo ciliogenesis upon a G1 arrest. Hence we treated RPE1 cells with NEK7 siRNA for 48 h and tested the frequency of ciliation compared with that of control cells after serum starvation for the same duration. To quantify ciliogenesis, we immunostained these cells with antibodies against acetylated tubulin (AcTub) and the intraflagellar transport protein IFT88, which mark both the cilium and centrioles (Figure 4, A and D). Astonishingly, we found that in NEK7-depleted cells, a high percentage of total RPE1 cells readily underwent ciliogenesis (Figure 4, A and B) and at approximately the same frequency as cells that had been grown in the absence of serum (~69% in serum-starved cells and ~67% in siNEK7 cells). This result suggests that the G1 arrest caused in siNEK7-treated cells may be very similar to what occurs in cells that have entered G0/G1 after a prolonged serum starvation and reinforces our hypothesis that NEK7 plays an important role in G1 progression, particularly for overcoming the restriction point.

In RPE1 cells, centriole duplication is usually inhibited upon serum starvation, as can be seen by the presence of only two centrin foci (Figure 4A). However, in the control experiments with serum starvation, we found that both STIL and SAS-6 were present around these mother centrioles in ~48% of all ciliated cells (Figure 4, C and D, and Supplemental Figure S6A), and centriolar recruitment of both STIL and SAS-6 appeared to be independent of the total expression levels of these proteins (Figure 4E). This suggests that recruitment of STIL and SAS-6 to the proximal part of mother centrioles is not entirely contingent upon the G1/S transition, unlike centriole duplication. On the other hand, in NEK7-depleted cells, we found that only ~12% of all ciliated cells exhibited centrioles with STIL and SAS-6 foci (Figure 4, C and D), even though the total protein levels of STIL and SAS-6 in NEK7-depleted cells were not significantly different from those in control serum-starved cells (Figure 4, C–E). In addition, we observed that PLK4 could also localize to the basal bodies under both of these conditions (Supplemental Figure S6B). This indicates that in NEK7-depleted cells, the G1 arrest may not be the sole reason for the defective recruitment of STIL and SAS-6 to the centrioles but that they may be regulated by NEK7 in another manner.

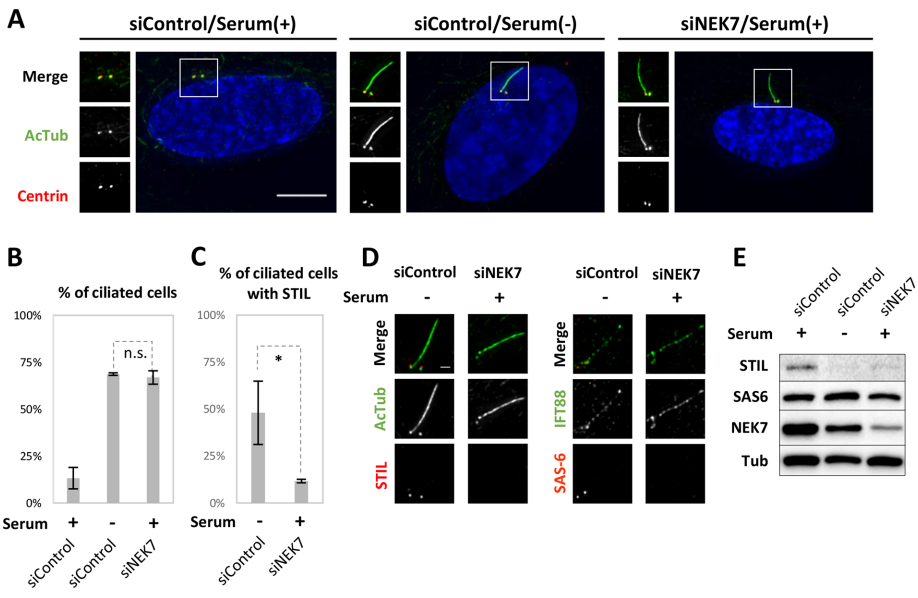

FIGURE 4: Depletion of NEK7 induces ciliogenesis. RPE1 cells were transfected with control and NEK7 siRNAs for a total of 48 h, and additional samples were simultaneously treated with a control siRNA and released into serum-free medium for a total of 48 h. (A) The cells were then fixed and stained with the indicated antibodies. DNA is shown in blue. Scale bar, 5 μm. (B) Percentage of interphase cells that were ciliated. (C) Percentage of ciliated cells that exhibited STIL foci at the basal bodies. More than 50 cells were counted in each experimental group. All histogram values are mean percentages ± SD from three independent experiments. *$p < 0.05$; n.s., not significant (one-tailed *t* test). (D) Magnified views of centriolar proteins at the base of cilia in the indicated cells. Cells were prepared as in A. Scale bar, 1 μm. (E) Total cell lysates in each condition were analyzed by immunoblotting against the indicated antibodies.

STIL is targeted for proteasomal degradation by the APC/C^{Cdh1} in NEK7-depleted cells

We demonstrate that the depletion of NEK7 induces a G1 arrest, and to a certain extent,

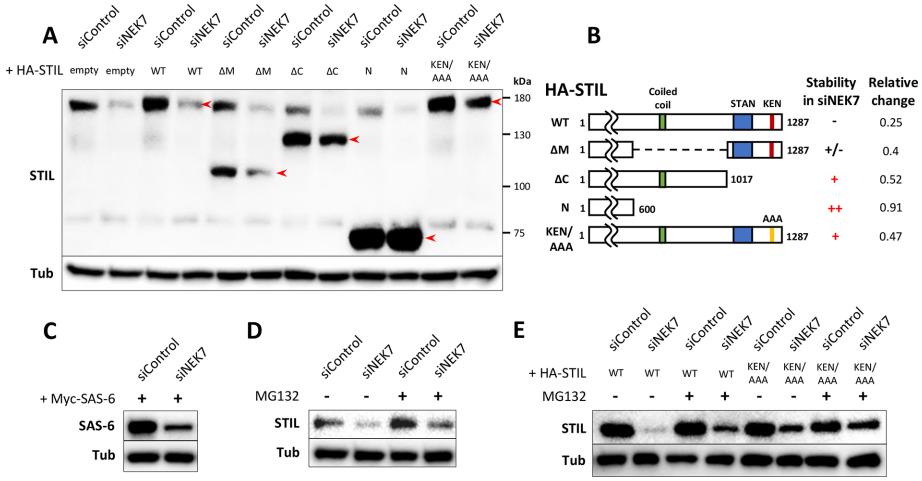

FIGURE 5: The centriolar protein STIL is targeted for proteasomal degradation by the APC/C^{Cdh1} in NEK7-depleted cells. (A, C) U2OS cells were transfected with control or NEK7 siRNAs for 24 h and then transfected with the indicated vectors for another 24 h. Total cell lysates were analyzed by immunoblotting using STIL, SAS-6, or tubulin antibodies. Right, approximate protein sizes in kilodaltons. Red arrowheads indicate expected bands for different constructs. (B) Schematic of the HA-STIL constructs used in A and E. WT, wild type; ΔM, Δ(601-1017); ΔC, Δ(1018-1287); N, Δ(601-1287). (D) U2OS cells were transfected with control or NEK7 siRNAs for 48 h, and 10 μM MG132 was added for the last 6 h of the siRNA treatment. (E) U2OS cells were treated as in A, and 10 μM MG132 was added to the last 6 h of the experiment.

this arrest explains the down-regulation of various procentriole proteins, such as STIL and SAS-6, that are expressed toward the G1/S transition (Erez *et al.*, 2008; Foster *et al.*, 2010). However, on the basis of the foregoing observation, we wondered whether the expression levels of these proteins were regulated in NEK7-depleted cells in a way other than transcriptional control. To test for possibilities other than transcriptional regulation, we overexpressed HA-STIL and Myc-SAS-6 constructs under the control of cytomegalovirus (CMV) promoters in NEK7-depleted cells to ensure their constitutive expression. Surprisingly, we found that even ectopically expressed STIL and SAS-6 exhibited reduced protein levels in the absence of NEK7 (Figure 5, A and C). In addition, upon overexpression of PLK4-Flag in NEK7-depleted cells, we found similarly reduced levels (Supplemental Figure S4). These results suggest that the levels of these proteins are regulated by a mechanism distinct from transcriptional control.

To check the stability of STIL in the absence of NEK7, we generated various deletion mutants of STIL in an effort to narrow the regions that may be responsible for its degradation (Figure 5, A and B). Among these mutants, the deletion of the C-terminal region spanning residues 1001–1287 (ΔC) largely rescued the low protein levels of STIL in NEK7-depleted cells. Upon narrowing the C-terminal region of STIL even further, we discovered that a triple alanine mutation of the KEN-box (KEN/AAA) in STIL was effective in rescuing the protein expression levels of ectopically expressed STIL (Figure 5, A and B). The KEN-box is the major recognition motif for the APC/C cofactor Cdh1 (Barford, 2011; Arquint and Nigg, 2014), and it is found in many proteins that are degraded by the APC/C^{Cdh1}-mediated ubiquitin-proteasomal pathway during late mitosis, including several centriolar proteins, such as SAS-6 and CPAP (Strnad *et al.*, 2007; Tang *et al.*, 2009). Because SAS-6 also contains a KEN-box, we also tested the stability of a KEN/AAA mutant of SAS-6 in NEK7-depleted cells but did not observe any rescue in expression (unpublished data). However, SAS-6 has been reported to be targeted by another E3 ubiquitin ligase during G1 (Puklowski *et al.*, 2011); it is therefore possible that this and possibly other, unidentified ubiquitin ligases may maintain the low cellular levels of SAS-6 in NEK7-depleted cells.

Our findings that the KEN/AAA mutant of STIL can be stably expressed even in the absence of NEK7 suggest that the down-regulation of STIL may partially be due to its ubiquitination by the APC/C^{Cdh1} and subsequent proteasomal degradation. To examine whether STIL undergoes active degradation by the proteasome in NEK7-depleted cells, we treated these cells with the proteasome inhibitor, MG132 (Figure 5, D and E). As expected, both endogenous and ectopically expressed STIL were partially rescued upon proteasomal inhibition, whereas the protein levels of the KEN/AAA mutant of STIL were not largely affected. We further tested the stability of the KEN/AAA mutant of STIL in vivo by using a PACT-tagged construct of STIL to artificially target it to the centrosomes (Gillingham and Munro, 2000). We found that the KEN/AAA mutant of PACT-STIL, but not wild-type PACT-STIL, could stably localize to the centrosomes (Supplemental Figure S5), suggesting that STIL may undergo localized degradation at the centrosomes via APC/C^{Cdh1} targeting. On the basis of these findings, we conclude that the down-regulation of STIL in NEK7-depleted cells is at least partly due to its ubiquitination by the APC/C^{Cdh1} and subsequent proteasomal degradation.

Cdh1 accumulates at centrosomes in the absence of NEK7

The APC/C^{Cdh1} is typically active from late mitosis to late G1 and plays a role in preventing premature DNA replication by regulating the levels of G1 cyclins as well as the CDK inhibitor p21 (Pines, 2011; Qiao *et al.*, 2014). Several feedback loops involving CDK-mediated phosphorylation of Cdh1 are necessary for the inactivation of APC/C^{Cdh1} at late G1, without which entry into the S-phase is blocked. On the basis of our previous results, we suspected that the APC/C^{Cdh1} may exist in an activated state in G1-arrested cells lacking NEK7 (Figures 1, 2, and 5). However, it is technically difficult to address the activation state of the APC/C^{Cdh1} in vivo. Instead, we tried to characterize whether Cdh1 might have altered expression patterns if NEK7 is depleted from cycling cells. First, overall Cdh1 expression levels were not affected on prolonged treatment of NEK7 siRNA (Figure 1G), even though the expression levels Cdc20 were low, which is a target of the APC/C^{Cdh1}. Next we looked at the localization patterns of Cdh1 within the cell. Cdh1 exists in both the cytoplasm and the nucleus and possibly shuttles between these two locations, depending on its phosphorylation status (Zhou *et al.*, 2003a,b). In *Drosophila* embryos, Cdh1/FZR1 has also been reported to localize to the centrosomes throughout the cell cycle (Raff *et al.*, 2002), and a recent study indicated that its centrosomal localization in *Drosophila* at least is cell cycle dependent (Meghini *et al.*, 2016). Of interest, when we looked at Cdh1 localization in control human U2OS cells, we also found that Cdh1 localized to the centrosomes throughout the cell cycle, and its localization followed a very specific pattern associated with cell cycle progression (Figure 6, A and B). In early G1, there appeared to be low levels of Cdh1 at the centrosomes, but as the cells continued into S and G2, Cdh1 gradually

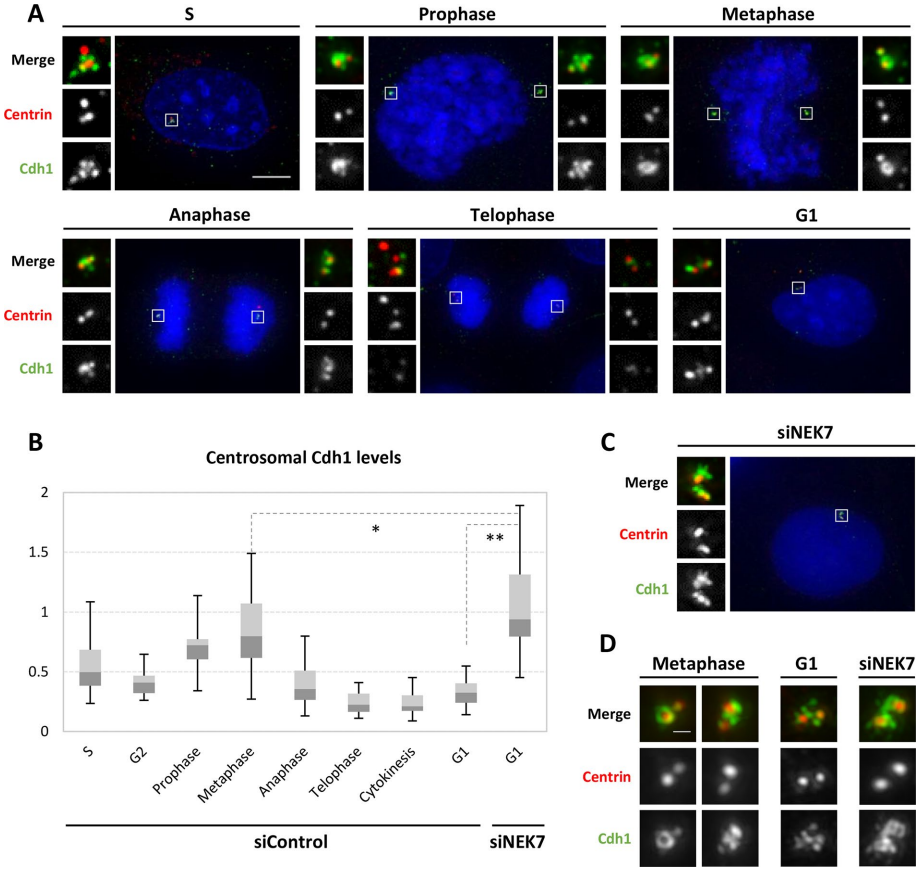

FIGURE 6: Localization patterns of the APC/C cofactor Cdh1 in control and NEK7-depleted cells. U2OS cells were transfected with control (A) or NEK7 (C) siRNAs for 48 h, and the cells were fixed and immunostained with antibodies specific to Cdh1 (green) and centrin (red). DNA is shown in blue. Insets are magnified views of the centrosomes. Scale bar, 5 μm. (B) The fluorescence intensities of Cdh1 at the centrosomes were quantified on an arbitrary scale at different cell cycle phases and are indicated as box plots. *$p < 0.05$; **$p < 0.01$ (one-tailed *t* test). (D) U2OS cells were imaged by 3D-SIM to address the localization of Cdh1 around the centrosomes. The fluorescence intensities of centrosomal Cdh1 are not comparable between images in D. Scale bar, 500 nm.

accumulated at the centrosomes. Cdh1 levels at the centrosomes peaked around prophase or metaphase, where it localized in small quantities at daughter centrioles and formed ring-like structures around mother centrioles. Immediately at the metaphase–anaphase transition, most of this Cdh1 disappeared from the centrosomes. We speculate that at this point, Cdh1 may relocalize to replace Cdc20 in the APC/C^{Cdc20} complex elsewhere in the cell, as APC/C^{Cdh1} activation and Cdc20 degradation are known to occur during this timeframe (Pines, 2011; Qiao *et al.*, 2014). We also observed small amounts of Cdh1 associated with centriolar satellites throughout the cell cycle, as indicated by the satellite marker PCM1 (Figure 6A and Supplemental Figure S7). Thus we report here for the first time that Cdh1 follows very specific localization patterns during the cell cycle in human cells, and we suspect that Cdh1 function and activity may be tied to its localization.

After characterization of Cdh1 localization patterns in control cells, we looked at Cdh1 in NEK7-depleted cells and found astoundingly high amounts of Cdh1 present at the centrosomes in U2OS cells (Figure 6, B and C, and Supplemental Figure S1B) but not in ciliated RPE1 cells (Supplemental Figure S6C). This centrosomal accumulation of Cdh1 in NEK7-depleted U2OS cells appeared to be quite different from the mitosis-specific accumulation in control cells. Hence we further examined the finer details of Cdh1 localization using three-dimensional structured illumination microscopy (3D-SIM). We found that whereas Cdh1 in control G1 cells did not show a specific localization pattern within the centrosomes, in control metaphase and NEK7-depleted cells, Cdh1 seemed to localize alongside the walls of mother centrioles (Figure 6D). Of interest, we observed that depletion of the centriolar satellite component PCM1 appeared to target high levels of Cdh1 to the centrosomes in similar patterns as seen in NEK7-depleted cells (Supplemental Figure S7, B and C), suggesting that centriolar satellites may play a role in Cdh1 localization.

At least in control cells, we wondered whether the mitotic accumulation of Cdh1 at the centrosomes might depend on the expansion of the PCM surrounding the centrioles. Organization of the PCM in interphase and mitotic centrosomes is inherently different; from early mitosis to metaphase, the PCM grows substantially in size for the formation of the mitotic spindle and then rapidly disassembles as the cells advance to anaphase. The core centrosomal protein CEP192 plays a major role in this process, as it is a crucial component for PCM assembly; depletion of CEP192 frequently results in the formation of disorganized spindles (Gomez-Ferreria *et al.*, 2007). When we coimmunostained control mitotic cells with Cdh1 and several centriolar markers, we found that the outer diameter of the Cdh1 ring was larger than that of CEP152, which is an inner PCM component, yet significantly smaller than that of CEP192 (Figure 7, A–C). On the basis of these data and past studies, we conclude that Cdh1 tends to accumulate in the inner to intermediate regions of the PCM (Lawo *et al.*, 2012; Sonnen *et al.*, 2012), which is consistent with a recent study on *Drosophila* Cdh1/FZR1 (Meghini *et al.*, 2016). Although CEP152 seemingly localizes closer to the centrosomes compared to Cdh1, depletion of CEP152 had no noticeable effect on Cdh1 localization (Supplemental Figure S8). To examine the PCM dependence of Cdh1 centrosomal localization, we depleted CEP192 in U2OS cells, and quantified the amount of Cdh1 present at the centrosomes in mitotic cells containing monopolar spindles, as well as in interphase cells (Figure 7, C, D, and F). Of interest, we found that although centrosomal levels of Cdh1 in interphase cells were unaffected upon CEP192 depletion, most of the mitotic accumulation of centrosomal Cdh1 was lost (Figure 7, D and F). This led us to hypothesize the existence of two independent populations of Cdh1 at the centrosomes; small quantities of Cdh1 are present at the centrosomes throughout the cell cycle and are independent of PCM assembly, whereas the mitotic accumulation of Cdh1 at the centrosomes appears to be largely PCM dependent.

We next sought to investigate whether Cdh1 accumulation at the centrosomes in the absence of NEK7 is PCM dependent as

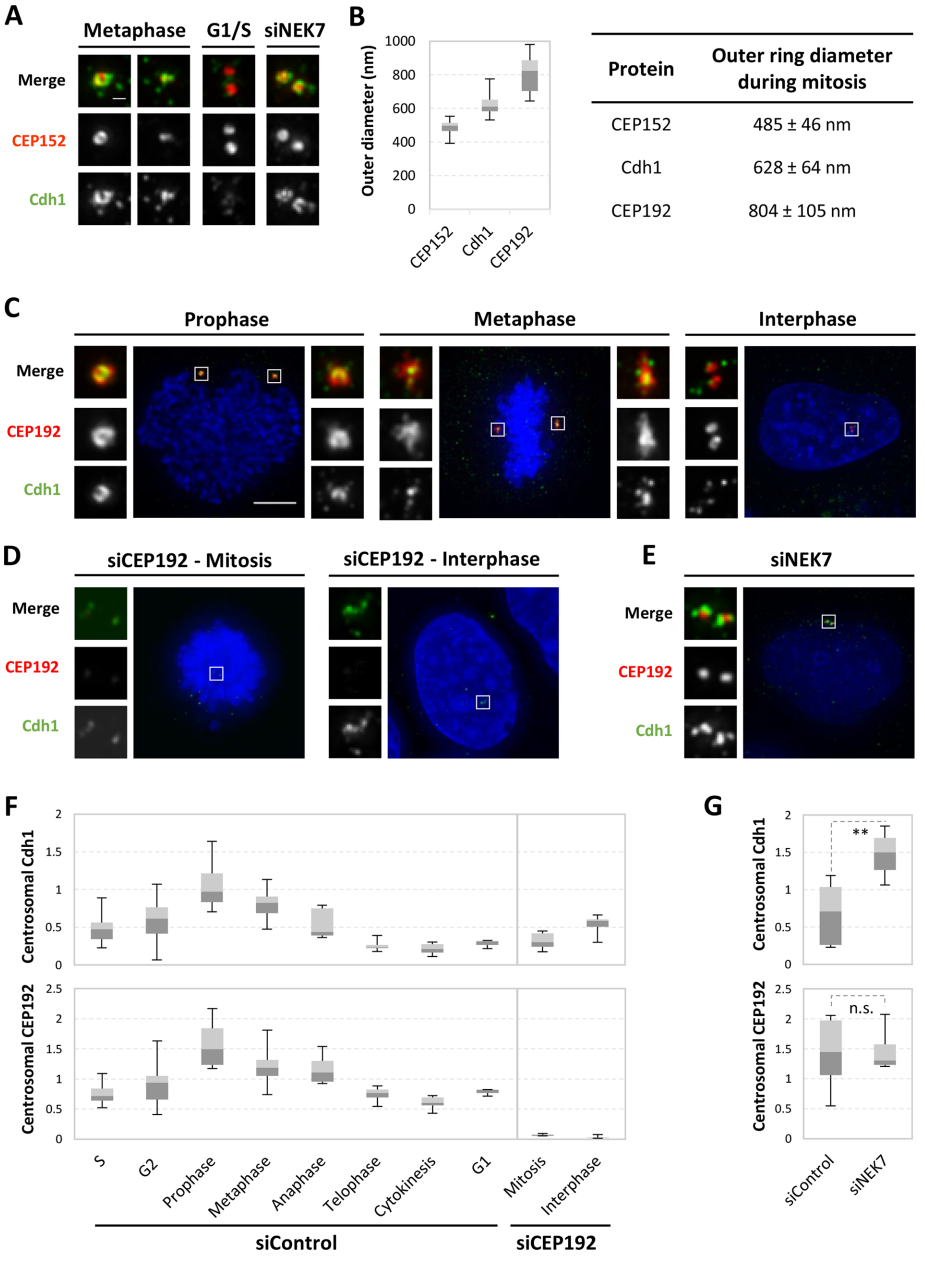

FIGURE 7: Centrosomal accumulation of Cdh1 in NEK7-depleted cells is PCM independent. U2OS cells were transfected with control (A, C), CEP192 (D), or NEK7 (A, E) siRNAs for 48 h, and the cells were fixed and immunostained with the indicated antibodies. DNA is shown in blue. Insets are magnified views of the centrosomes. Scale bars, 500 nm (A), 5 μm (C). (B) Approximate outer diameters of the indicated proteins at mitotic centrosomes. (F, G) Fluorescence intensities of Cdh1 and CEP192 at the centrosomes were quantified on an arbitrary scale at different cell cycle phases and are indicated as box plots. $^{**}p < 0.01$; n.s., not significant (one-tailed *t* test).

well. To do so, we compared the amounts of CEP192 and Cdh1 at the centrosomes during interphase in control and NEK7 siRNA–treated cells (Figure 7, E and G). Similar to a previous study that reported a slight loss in the PCM content in NEK7-depleted cells (Kim *et al.*, 2011), we found no significant increase in the amounts of CEP192 present at the centrosomes, even though Cdh1 levels were elevated (Figure 7G). This result suggests that Cdh1 accumulation at the centrosomes in the absence of NEK7 is PCM independent and possibly recruited by other, unknown pathways to inhibit centriole duplication.

DISCUSSION

NEK7 is required for many different cellular processes, suggesting that it acts on and regulates many different substrates and may itself lie under complex cell cycle control. A recent study identified many different interactors of NEK7 using a proteomics-based approach, and these proteins were found to be involved in several other processes not previously reported for NEK7, such as mitochondrial regulation, intracellular protein transport, and DNA repair (de Souza *et al.*, 2014). It was also shown that NEK7 could phosphorylate several of its binding partners, suggesting that it acts as a multifunctional kinase (de Souza *et al.*, 2014). However, the specific roles of NEK7 and NEK7-mediated phosphorylation events in the cell cycle have not been identified, making it difficult to clarify the significance of NEK7 in specific biological processes. In our study, we attempted to characterize the effect of NEK7 on cell cycle progression by analyzing the effects of NEK7 depletion in cycling cells. Here we propose that NEK7 plays crucial roles in the expression and stability of various G1 proteins, as well as in the regulation of APC/C^{Cdh1} activity and localization, both of which contribute to timely transition from the G1 to the S-phase. Our results demonstrate that NEK7 may play an integral and indispensable role in progression through the G1 phase and subsequent commitment to the rest of the cell cycle.

During G1 progression in cycling cells, the expression levels of various cyclins and activity levels of cyclin–CDK complexes determine whether the cells will proliferate or become quiescent (Figure 8). Another factor that affects this decision is the ubiquitin ligase APC/C^{Cdh1}, which regulates the expression levels of cyclins and other regulatory proteins in intricately linked feedback loops. Concomitant with the decision to enter the cell cycle, centriole duplication is initiated, and this process is also under the control of the cell cycle. In our study, we show that NEK7 is required for the timely expression of various cyclins, CDKs, and other cell cycle–regulated proteins; in the absence of these cyclin–CDK complexes, cells lacking NEK7 are inevitably arrested in the G1 phase, presumably before they can pass the restriction point (Figure 8). APC/C^{Cdh1} also appears to remain active in NEK7-depleted cells, and the inhibition of APC/C^{Cdh1} inactivation may further contribute to the G1 arrest (Pines, 2011; Qiao *et al.*, 2014). Based on the data, it is tempting to speculate on the earliest targets of NEK7 in the cell cycle or the pathways in which it might be involved. The most-upstream protein to be affected in the absence of NEK7 is cyclin D1 (Figures 1D and 8), which exhibited reduced expression levels even in early G1 in NEK7-depleted cells. Mitogen-activated protein kinase (MAPK)–mediated signaling is perhaps the best-studied activator of cyclin D1 gene expression

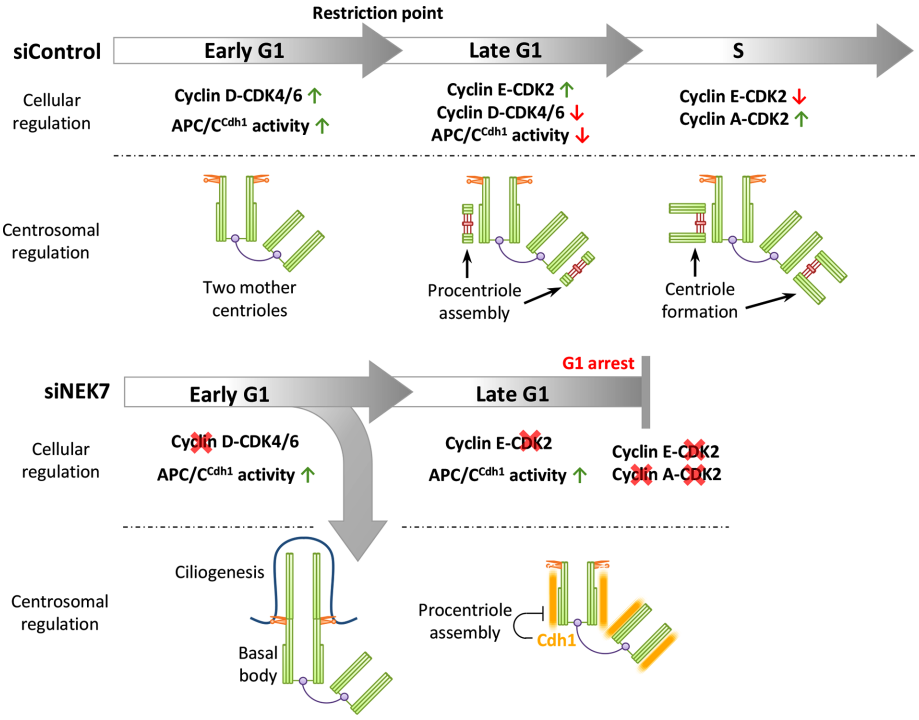

FIGURE 8: Depletion of NEK7 inhibits G1 progression and centriole duplication. (Top) Schematic of how progression through G1 and the G1/S transition is regulated in control cells. During early G1, increases in cyclin D–CDK4/6 activity are necessary to pass the restriction point, and these complexes are subsequently inactivated in late G1. The G1/S transition largely depends on cyclin E/CDK2 activity, and inactivation of the APC/C^{Cdh1} is essential for S-phase entry. At the same time, various procentriolar proteins are expressed that are required for the initiation of centriole duplication. Toward S-phase, cyclin A replaces cyclin E in the complex with CDK2 to complete DNA replication, and procentriole assembly is completed as well. (Bottom) In the absence of NEK7, the expression of various cyclins is inhibited; in particular, expression of the early G1 cyclin D is blocked. Low levels of cyclin D could lead to an arrest at the restriction point, which induces ciliogenesis. In the absence of cyclin D–CDK4/6 activity, expression of late G1 cyclins and CDKs is also reduced. In addition, inactivation of the APC/C^{Cdh1} is also inhibited, and these aberrant conditions cause a G1 arrest in NEK7-depleted cells. Cdh1 also accumulates at the centriole walls in these cells, which may inhibit procentriole formation.

(Klein and Assoian, 2008) during early G1, suggesting that NEK7 may play a role in at least one or more of the growth factor signaling pathways regulating the transcriptional activation of cyclin D1. Further evidence for NEK7 being involved in growth factor–mediated signaling is the formation of primary cilia in NEK7-depleted RPE1 cells, a phenotype that is characteristic of cells arrested in G0/G1 upon serum starvation (Figures 4 and 8). Another signaling network that may be affected by NEK7 is the mammalian target of rapamycin (mTOR) pathway, which plays a complex role in G1 progression by regulating cyclin E–CDK2 activity levels (Foster *et al.*, 2010). Indeed, one of the few identified substrates of NEK7 is p70S6K (Belham *et al.*, 2001), a ribosomal protein kinase that functions in the mTOR signaling pathway and promotes protein synthesis and cell proliferation upon activation. Although not much is known about transcriptional regulation of the CDK2 gene, our results suggest that NEK7 may function upstream of CDK2 gene transcription, or it may directly or indirectly regulate CDK2 protein stability (Figures 1, 2, and 8).

A particularly interesting phenotype that we observed was the localization pattern of Cdh1 at the centrosomes during the cell cycle, especially the high accumulation of Cdh1 at the centrosomes in NEK7-depleted cells (Figures 6–8). These results raise important questions about the significance and functions of centrosomal Cdh1. One obvious question is whether Cdh1 exists in a complex with the APC/C at the centrosomes, and, if so, whether centrosomal APC/C^{Cdh1} is active or inactive. The protein Emi1, which can bind to and inhibit both APC/C activators Cdc20 and Cdh1 (Reimann *et al.*, 2001; Miller *et al.*, 2006), localizes to the spindle pole in a complex with the APC/C during early mitosis (Ban *et al.*, 2007) and inhibits centrosomal APC/C to prevent degradation of spindle pole–associated cyclins and premature mitotic exit. Hence we speculate that the PCM-associated Cdh1 seen during mitosis is likely kept inactive in a complex with the APC/C and Emi1, after chromosome segregation and activation of APC/C^{Cdh1}, it is possible that it disperses throughout the cytoplasm to target various substrates, which may explain the disappearance of Cdh1 from the centrosomes. In the next cell cycle, APC/C^{Cdh1} remains active until the G1/S transition, in which Emi1 stably binds and irreversibly inactivates APC/C^{Cdh1} to commit cells to enter the cell cycle (Hsu *et al.*, 2002; Machida and Dutta, 2007; Cappell *et al.*, 2016).

An important implication of our study is that the unusually high levels of centrosomal Cdh1 in NEK7-depleted cells represent active APC/C^{Cdh1} as well, as these cells have been arrested in G1. This raises several important possibilities. The centrosomes have long been recognized as hubs for localized proteasomal degradation of ubiquitinated proteins (Fisk, 2012). Thus it is possible that centrosomal APC/C^{Cdh1} in G1-arrested cells serves to rapidly mark various substrates for destruction to prevent proliferation. Another possible function of centrosomal APC/C^{Cdh1} may be to inhibit centriole duplication (Figure 8), as it could potentially occupy and block the assembly sites of new procentrioles. Thus APC/C^{Cdh1} could perform several functions at the centrosomes in G1-arrested cells lacking NEK7. However, how this complex is recruited to the centrosomes in these particular conditions remains to be addressed.

In conclusion, our study strongly suggests that NEK7 is an important kinase involved in the regulation of G1-phase progression and the G1/S transition. In the future, it would be worthwhile to identify and characterize the direct downstream targets of NEK7, as well as the pathways in which it plays an important role. Because NEK7 has already been reported to be up-regulated in various cancers (Wang *et al.*, 2013; Saloura *et al.*, 2015; Kooi *et al.*, 2016; Zhou *et al.*, 2016), the strong G1 arrest that is induced upon NEK7 depletion makes it a promising candidate for the development of anticancer drugs.

MATERIALS AND METHODS

Cell culture and transfection

Human U2OS cells were obtained from the European Collection of Authenticated Cell Cultures (ECACC) and were authenticated by STR profiling in ECACC. Telomerase-immortalized human RPE1 (hTERT-RPE1) cells were obtained from Clontech. U2OS and RPE1 cells were cultured in DMEM and DMEM: Nutrient Mixture F-12 (DMEM/F-12), respectively, supplemented with 10% fetal bovine

serum (FBS) and penicillin/streptomycin at 37°C in a 5% CO_2 incubator. The lines were mycoplasma free, as confirmed by Hoechst 33258 staining. Transfection of siRNA or DNA constructs into U2OS and RPE1 cells was performed using Lipofectamine RNAiMAX (Life Technologies) or Lipofectamine 2000 (Life Technologies) according to the manufacturer's instructions. Unless otherwise noted, transfected cells were analyzed 48 h after transfection with siRNA and 24 h after transfection with DNA constructs.

RNA interference and plasmids

The following siRNAs were used: Silencer Select siRNA (Life Technologies) against the CDS of NEK7 (s44316), CEP192 (s226819), and PCM1 (s10128 and s10129). Custom siRNAs were used against the 3′ untranslated region of NEK7 (5′-GCA UUU GUA AAC UUA AAA ATT-3′) and the CDS of CEP152 (5′-GCG GAU CCA ACU GGA AAU CUA TT-3′).

The following plasmids were used: pFlag-NEK7 RR (subcloned from the pFlag-CMV2-NEK7 vector, a gift from Andrew M. Fry, University of Leicester, UK), pEBTet-GFP-STIL, pcDNA3-PLK4-ΔPEST-Flag (a gift from Hiroyuki Mano, University of Tokyo, Japan), pCMV5-HA-STIL WT, and pCMV5-Myc-SAS-6. pCMV5-HA-STIL constructs were subcloned from the pCMV5-HA-STIL WT vector using PrimeSTAR mutagenesis basal kit (TaKaRa).

Cell cycle synchronization and flow cytometric analysis

For cell synchronization at prometaphase, cells were treated with 100 ng/ml nocodazole for 16 h and released in fresh medium. For cell synchronization at S-phase, cells were treated with 2 mM thymidine for 16 h and released in fresh medium. For flow cytometric analyses, cells cultured on dishes were trypsinized, washed twice with phosphate-buffered saline (PBS), and fixed in 70% cold ethanol at −20°C for >3 h. The fixed cells were then washed with PBS and incubated with Muse Cell Cycle Reagent at room temperature for 30 min. The DNA contents of the cells were then measured using Muse Cell Analyzer (Merck Millipore).

Antibodies

The following primary antibodies were used in this study: rabbit polyclonal antibodies against STIL (ab89314; Abcam; immunofluorescence [IF], 1:500; immunoblotting [IB], 1:1000), green fluorescent protein (598; MBL; IF 1:500), NEK7 (A302-684A; Bethyl Laboratories; IB, 1:1000), centrin-1 (ab11257; Abcam; IF, 1:500), CPAP/CENP-J (11517-1-AP; Proteintech; IF, 1:500; IB, 1:1000), Cdc20 (A301-180A; Bethyl Laboratories; IB, 1:500), IFT88 (13967-1-AP; Proteintech; IF, 1:100), CEP192 (A302-324A; Bethyl Laboratories; IF, 1:500), CEP152 (A302-324A; Bethyl Laboratories; IF, 1:500), HA tag (ab9110; Abcam; IF, 1:500), PCM1 (HPA023370; Sigma-Aldrich; IF 1:500); mouse monoclonal antibodies against p21 Waf1/Cip1 (DCS60; Cell Signaling Technology; IF, 1:500; IB, 1:1000; a gift from Masato Kanemaki, National Institute of Genetics, Japan), centrin-2 (20H5; Millipore; IF, 1:1000), SAS-6 (sc-81431; Santa Cruz Biotechnology; WB, 1:1000), PLK4 (clone 6H5, MABC544; Merck Millipore; IF, 1:300), Flag tag (F1804; Sigma-Aldrich; IF, 1:1000; WB, 1:1000), Cdh1/FZR1 (ab89535; Abcam; IF, 1:100; WB, 1:500), acetylated α-tubulin at K40 (611B1; Sigma-Aldrich; IF, 1:500), and α-tubulin (DM1A; Sigma-Aldrich; WB, 1:2000). The CDK and cyclin antibodies were used from the CDK and Cyclin Antibody Sampler Kits (9868 and 9869, respectively; Cell Signaling Technology) as per recommended dilutions. The following secondary antibodies were used: Alexa Fluor 488 goat anti-mouse immunoglobulin G (IgG; H+L; 1:500; Molecular Probe), Alexa Fluor 568 goat anti-rabbit IgG (H+L; 1:500; Molecular Probe) for IF; and goat polyclonal antibody–horseradish peroxidase (HRP) against mouse IgG (W402B; Promega; 1:10,000) and rabbit IgG (W401B; Promega; 1:10,000) for WB. Centrin-1 (rabbit) and centrin-2 (mouse) antibodies were used as centriolar markers. Acetylated α-tubulin at K40 (mouse) and IFT88 (rabbit) antibodies were used as ciliary markers.

Immunofluorescence

For indirect immunofluorescence microscopy, cells cultured on coverslips were fixed using ice-cold methanol for 10 min at −20°C. The cells were then washed with PBS thrice and incubated for blocking with 1% BSA in PBS/0.5% Triton X-100 (PBSX) for 30 min at room temperature. The cells were then incubated with primary antibodies for 3 h at room temperature, washed with PBSX once and PBS three times, and incubated with secondary antibodies for 1 h at room temperature. The cells were thereafter washed with PBSX twice, stained with 0.2 μg/ml Hoechst 33258 in PBS for 5 min at room temperature, washed again with PBS, and mounted onto glass slides.

Counting of immunofluorescence signals was performed using an Axioplan2 fluorescence microscope (Carl Zeiss) with a 100×/1.4 numerical aperture (NA) Plan-Apochromat objective. Data acquisition for the images was performed using a DeltaVision Personal DV-SoftWoRx system (Applied Precision) equipped with a CoolSNAP CH350 charge-coupled device (CCD) camera. The images were acquired as serial sections along the *Z*-axis and stacked using the "quick projection" algorithm in SoftWoRx. The signal intensities for centrosomal proteins were quantified using the Data Inspector tool in SoftWoRx. The captured images were processed using ImageJ. Unless otherwise noted, all immunofluorescence analyses were repeated at least three times.

The 3D-SIM images were taken by the Nikon N-SIM imaging system with piezo stage, Apo TIRF 100× oil objective lens (NA 1.49), excitation wavelengths of 488 and 561 nm, and iXon DU-897 electron-multiplying CCD camera (Andor Technology). The images were collected at 100-nm *Z*-steps.

Immunoblotting

For preparation of cell lysates for immunoblotting, the cells were collected and lysed by vortexing at 4°C in lysis buffer (20 mM Tris/HCl, pH 7.5, 100 mM NaCl, 0.5% NP-40, 1 mM EDTA, 1 mM dithiothreitol, and 1/1000 protease 26 inhibitor cocktail (Nacalai Tesque). Lysates were cleared by centrifugation for 10 min at 13,000 rpm at 4°C, and the supernatants were collected for immunoblotting. SDS–PAGE was performed using 6–12% polyacrylamide gels, followed by transfer on Immobilon-P membrane (Millipore). The membranes were probed with the primary antibodies, followed by incubation with their respective HRP-conjugated secondary antibodies (Promega). Washes were performed in PBS containing 0.02% Tween. The signals were detected by a Chemi Doc XRS+ (Bio-Rad), and band intensities were calculated using the inbuilt Image Lab software (Bio-Rad). Unless otherwise specified, all immunoblotting analyses were repeated at least three times. The antibody against α-tubulin was used as a loading control.

ACKNOWLEDGMENTS

We thank Daisuke Takao for critical reading of the manuscript, as well as members of the Kitagawa laboratory for fruitful discussions. This work was supported by a Grant-in-Aid for Young Scientists (A) and for Scientific Research on Innovative Areas from the Ministry of Education, Science, Sports and Culture of Japan, the Uehara Memorial Foundation, the Takeda Science Foundation, and the Naito Foundation.

REFERENCES

Abbas T, Dutta A (2009). p21 in cancer: intricate networks and multiple activities. Nat Rev Cancer 9, 400–414.

Arquint C, Nigg EA (2014). STIL microcephaly mutations interfere with APC/C-mediated degradation and cause centriole amplification. Curr Biol 24, 351–360.

Arquint C, Sonnen KF, Stierhof YD, Nigg EA (2012). Cell-cycle-regulated expression of STIL controls centriole number in human cells. J Cell Sci 125, 1342–1352.

Ayeni JO, Campbell SD (2014). "Ready, set, go": checkpoint regulation by Cdk1 inhibitory phosphorylation. Fly 8, 140–147.

Ban KH, Torres JZ, Miller JJ, Mikhailov A, Nachury MV, Tung JJ, Rieder CL, Jackson PK (2007). The END network couples spindle pole assembly to inhibition of the anaphase-promoting complex/cyclosome in early mitosis. Dev Cell 13, 29–42.

Barford D (2011). Structural insights into anaphase-promoting complex function and mechanism. Philos Trans R Soc Lond Biol Sci 1584, 3605–3624.

Barr AR, Heldt FS, Zhang T, Bakal C, Novak B (2016). A dynamical framework for the all-or-none G1/S transition. Cell Syst 2, 27–37.

Belham C, Comb MJ, Avruch J (2001). Identification of the NIMA family kinases NEK6/7 as regulators of the p70 ribosomal S6 kinase. Curr Biol 11, 1155–1167.

Bertoli C, Skotheim JM, de Bruin RAM (2013). Control of cell cycle transcription during G1 and S phases. Nat Rev Mol Cell Biol 14, 518–528.

Cappell SD, Chung M, Jaimovich A, Spencer SL, Meyer T (2016). Irreversible APC(Cdh1) inactivation underlies the point of no return for cell-cycle entry. Cell 166, 167–180.

Cunha-Ferreira I, Bento I, Pimenta-Marques A, Jana SC, Lince-Faria M, Duarte P, Borrego-Pinto J, Gilberto S, Amado T, Brito D, *et al.* (2013). Regulation of autophosphorylation controls PLK4 self-destruction and centriole number. Curr Biol 23, 2245–2254.

Cunha-Ferreira I, Rodrigues-Martins A, Bento I, Riparbelli M, Zhang W, Laue E, Callaini G, Glover DM, Bettencourt-Dias M (2009). The SCF/Slimb ubiquitin ligase limits centrosome amplification through degradation of SAK/PLK4. Curr Biol 19, 43–49.

De Boer L, Oakes V, Beamish H, Giles N, Stevens F, Somodevilla-Torres M, DeSouza C, Gabrielli B (2008). Cyclin A/cdk2 coordinates centrosomal and nuclear mitotic events. Oncogene 27, 4261–4268.

de Souza EE, Meirelles GV, Godoy BB, Perez AM, Smetana JHC, Doxsey SJ, McComb ME, Costello CE, Whelan Sa, Kobarg J (2014). Characterization of the human NEK7 interactome suggests catalytic and regulatory properties distinct from those of NEK6. J Proteome Res 13, 4074–4090.

Dzhindzhev NS, Tzolovsky G, Lipinszki Z, Schneider S, Lattao R, Fu J, Debski J, Dadlez M, Glover DM (2014). Plk4 phosphorylates Ana2 to trigger Sas6 recruitment and procentriole formation. Curr Biol 24, 2526–2532.

Erez A, Chaussepied M, Castiel A, Colaizzo-Anas T, Aplan PD, Ginsberg D, Izraeli S (2008). The mitotic checkpoint gene, SIL is regulated by E2F1. Int J Cancer 123, 1721–1725.

Fischer M, Quaas M, Wintsche A, Müller GA, Engeland K (2014). Polo-like kinase 4 transcription is activated via CRE and NRF1 elements, repressed by DREAM through CDE/CHR sites and deregulated by HPV E7 protein. Nucleic Acids Res 42, 163–180.

Fisk HA (2012). Many pathways to destruction: the role of the centrosome in, and its control by regulated proteolysis. In: The Centrosome, Totowa, NJ: Humana Press, 133–155.

Foster D, Yellen P, Xu L, Saqcena M (2010). Regulation of G1 cell cycle progression: distinguishing the restriction point from a nutrient-sensing cell growth checkpoint(s). Genes Cancer 1, 1124–1131.

Fry AM, O'Regan L, Sabir SR, Bayliss R (2012). Cell cycle regulation by the NEK family of protein kinases. J Cell Sci 125, 4423–4433.

Gillingham AK, Munro S (2000). The PACT domain, a conserved centrosomal targeting motif in the coiled-coil proteins AKAP450 and pericentrin. EMBO Rep 1, 524–529.

Gomez-Ferreria MA, Rath U, Buster DW, Chanda SK, Caldwell JS, Rines DR, Sharp DJ (2007). Human Cep192 is required for mitotic centrosome and spindle assembly. Curr Biol 17, 1960–1966.

Gong D, Ferrell JE Jr (2010). The roles of cyclin A2, B1, and B2 in early and late mitotic events. Mol Biol Cell 21, 3149–3161.

Grim JE, Gustafson MP, Hirata RK, Hagar AC, Swanger J, Welcker M, Hwang HC, Ericsson J, Russell DW, Clurman BE (2008). Isoform- and cell cycle-dependent substrate degradation by the Fbw7 ubiquitin ligase. J Cell Biol 181, 913–920.

Guderian G, Westendorf J, Uldschmid A, Nigg EA (2010). Plk4 trans-autophosphorylation regulates centriole number by controlling beta TrCP-mediated degradation. J Cell Sci 4, 2163–2169.

Habedanck R, Stierhof Y-D, Wilkinson CJ, Nigg EA (2005). The Polo kinase Plk4 functions in centriole duplication. Nat Cell Biol 7, 1140–1146.

Harrison MK, Adon AM, Saavedra HI (2011). The G1 phase Cdks regulate the centrosome cycle and mediate oncogene-dependent centrosome amplification. Cell Div 6, 2.

Hsu JY, Reimann JDR, Sørensen CS, Lukas J, Jackson PK (2002). E2F-dependent accumulation of hEmi1 regulates S phase entry by inhibiting APC(Cdh1). Nat Cell Biol 4, 358–366.

Kim S, Kim S, Rhee K, Kim S (2011). NEK7 is essential for centriole duplication and centrosomal accumulation of pericentriolar material proteins in interphase cells. J Cell Sci 124, 3760–3770.

Kim S, Lee K, Rhee K (2007). NEK7 is a centrosomal kinase critical for microtubule nucleation. Biochem Biophys Res Commun 360, 56–62.

Klebba JE, Buster DW, McLamarrah TA, Rusan NM, Rogers GC (2015a). Autoinhibition and relief mechanism for Polo-like kinase 4. Proc Natl Acad Sci USA 112, E657–E666.

Klebba JE, Buster DW, Nguyen AL, Swatkoski S, Gucek M, Rusan NM, Rogers GC (2013). Polo-like kinase 4 autodestructs by generating its Slimb-binding phosphodegron. Curr Biol 23, 2255–2261.

Klebba JE, Galletta BJ, Nye J, Plevock KM, Buster DW, Hollingsworth Na, Slep KC, Rusan NM, Rogers GC (2015b). Two Polo-like kinase 4 binding domains in Asterless perform distinct roles in regulating kinase stability. J Cell Biol 208, 401–414.

Klein EA, Assoian RK (2008). Transcriptional regulation of the cyclin D1 gene at a glance. J Cell Sci 121, 3853–3857.

Kleylein-Sohn J, Westendorf J, Le Clech M, Habedanck R, Stierhof YD, Nigg EA (2007). Plk4-induced centriole biogenesis in human cells. Dev Cell 13, 190–202.

Kooi IE, Mol BM, Massink, MPG, de Jong MC, de Graaf P, van der Valk P, Meijers-Heijboer H, Kaspers GJL, Moll AC, te Riele H, *et al.* (2016). A meta-analysis of retinoblastoma copy numbers refines the list of possible driver genes involved in tumor progression. PLoS One 11, e0153323.

Kratz A-S, Bärenz F, Richter KT, Hoffmann I (2015). Plk4-dependent phosphorylation of STIL is required for centriole duplication. Biol Open 4, 370–377.

Lawo S, Hasegan M, Gupta GD, Pelletier L (2012). Subdiffraction imaging of centrosomes reveals higher-order organizational features of pericentriolar material. Nat Cell Biol 14, 1148–1158.

Leidel S, Delattre M, Cerutti L, Baumer K, Gönczy P (2005). SAS-6 defines a protein family required for centrosome duplication in C. elegans and in human cells. Nat Cell Biol 7, 115–125.

Machida YJ, Dutta A (2007). The APC/C inhibitor, Emi1, is essential for prevention of rereplication. Genes Dev 21, 184–194.

Masamha CP, Benbrook DM (2009). Cyclin D1 degradation is sufficient to induce G1 cell cycle arrest despite constitutive expression of cyclin E2 in ovarian cancer cells. Cancer Res 69, 6565–6572.

Meghini F, Martins T, Tait X, Fujimitsu K, Yamano H, Glover DM, Kimata Y (2016). Targeting of Fzr/Cdh1 for timely activation of the APC/C at the centrosome during mitotic exit. Nat Commun 7, 12607.

Miller JJ, Summers MK, Hansen DV, Nachury MV, Lehman NL, Loktev A, Jackson PK (2006). Emi1 stably binds and inhibits the anaphase-promoting complex/cyclosome as a pseudosubstrate inhibitor. Genes Dev 20, 2410–2420.

Moyer TC, Clutario KM, Lambrus BG, Daggubati V, Holland AJ (2015). Binding of STIL to Plk4 activates kinase activity to promote centriole assembly. J Cell Biol 209, 863–878.

Musacchio A, Salmon ED (2007). The spindle-assembly checkpoint in space and time. Nat Rev Mol Cell Biol 8, 379–393.

Narasimha A, Kaulich M, Shapiro G, Choi YJ, Sicinski P, Dowdy SF (2014). Cyclin D activates the Rb tumor suppressor by mono-phosphorylation. Elife 3, 10.7554/eLife.02872.

Ohta M, Ashikawa T, Nozaki Y, Kozuka-Hata H, Goto H, Inagaki M, Oyama M, Kitagawa D (2014). Direct interaction of Plk4 with STIL ensures formation of a single procentriole per parental centriole. Nat Commun 5, 5267.

Pines J (2011). Cubism and the cell cycle: The many faces of the APC/C. Nat Rev Mol Cell Biol 12, 427–438.

Puklowski A, Homsi Y, Keller D, May M, Chauhan S, Kossatz U, Grünwald V, Kubicka S, Pich A, Manns MP, *et al.* (2011). The SCF-FBXW5 E3-ubiquitin ligase is regulated by PLK4 and targets HsSAS-6 to control centrosome duplication. Nat Cell Biol 13, 1004–1009.

Qiao X, Zhang L, Gamper AM, Fujita T, Wan Y (2014). APC/C-Cdh1: from cell cycle to cellular differentiation and genomic integrity. Cell Cycle 9, 3904–3912.

Raff JW, Jeffers K, Huang J-Y (2002). The roles of Fzy/Cdc20 and Fzr/Cdh1 in regulating the destruction of cyclin B in space and time. J Cell Biol 157, 1139–1149.

Regan LO, Fry AM (2009). The Nek6 and Nek7 protein kinases are required for robust mitotic spindle formation and cytokinesis. Mol Cell Biol 29, 3975–3990.
Reimann JD, Gardner BE, Margottin-Goguet F, Jackson PK (2001). Emi1 regulates the anaphase-promoting complex by a different mechanism than Mad2 proteins. Genes Dev 15, 3278–3285.
Salem H, Rachmin I, Yissachar N, Cohen S, Amiel A, Haffner R, Lavi L, Motro B (2010). Nek7 kinase targeting leads to early mortality, cytokinesis disturbance and polyploidy. Oncogene 29, 4046–4057.
Saloura V, Cho HS, Kiyotani K, Alachkar H, Zuo Z, Nakakido M, Tsunoda T, Seiwert T, Lingen M, Licht J, *et al.* (2015). WHSC1 promotes oncogenesis through regulation of NIMA-related kinase-7 in squamous cell carcinoma of the head and neck. Mol Cancer Res 13, 293–304.
Schmidt TI, Kleylein-Sohn J, Westendorf J, Le Clech M, Lavoie SB, Stierhof Y-D, Nigg Ea (2009). Control of centriole length by CPAP and CP110. Curr Biol 19, 1005–1011.
Sonnen KF, Gabryjonczyk A-M, Anselm E, Stierhof Y-D, Nigg EA (2013). Human Cep192 and Cep152 cooperate in Plk4 recruitment and centriole duplication. J Cell Sci 126, 3223–3233.
Sonnen KF, Schermelleh L, Leonhardt H, Nigg EA (2012). 3D-structured illumination microscopy provides novel insight into architecture of human centrosomes. Biol Open 1, 965–976.
Strnad P, Gönczy P (2008). Mechanisms of procentriole formation. Trends Cell Biol 18, 389–396.
Strnad P, Leidel S, Vinogradova T, Euteneuer U, Khodjakov A, Gönczy P (2007). Regulated HsSAS-6 levels ensure formation of a single procentriole per centriole during the centrosome duplication cycle. Dev Cell 13, 203–213.
Tang C-JC, Fu R-H, Wu KS, Hsu W-B, Tang TK (2009). CPAP is a cell-cycle regulated protein that controls centriole length. Nat Cell Biol 11, 825–831.
Tang CC, Lin S, Hsu W, Lin Y, Wu C, Lin Y, Chang C, Wu K, Tang TK (2011). The human microcephaly protein STIL interacts with CPAP and is required for procentriole formation. EMBO J 30, 4790–4804.
Vulprecht J, David A, Tibelius A, Castiel A, Konotop G, Liu F (2007). STIL is required for centriole duplication in human cells. J Cell Sci 125, 1353–1362.
Wang G, Jiang Q, Zhang C (2014). The role of mitotic kinases in coupling the centrosome cycle with the assembly of the mitotic spindle. J Cell Sci 127, 4111–4122.
Wang R, Song Y, Xu X, Wu Q, Liu C (2013). The expression of Nek7, FoxM1, and Plk1 in gallbladder cancer and their relationships to clinicopathologic features and survival. Clin Transl Oncol 15, 626–632.
Yissachar N, Salem H, Tennenbaum T, Motro B (2006). Nek7 kinase is enriched at the centrosome, and is required for proper spindle assembly and mitotic progression. FEBS Lett 580, 6489–6495.
Zhou L, Wang Z, Xu X, Wan Y, Qu K, Fan H, Chen Q, Sun X, Liu C (2016). Nek7 is overexpressed in hepatocellular carcinoma and promotes hepatocellular carcinoma cell proliferation in vitro and in vivo. Oncotarget 7, 18620–18630.
Zhou Y, Ching Y-P, Chun ACS, Jin D-Y (2003a). Nuclear localization of the cell cycle regulator CDH1 and its regulation by phosphorylation. J Biol Chem 278, 12530–12536.
Zhou Y, Ching Y-P, Ng RWM, Jin D-Y (2003b). Differential expression, localization and activity of two alternatively spliced isoforms of human APC regulator CDH1. Biochem J 374, 349–358.
Zitouni S, Francia ME, Leal F, Montenegro Gouveia S, Nabais C, Duarte P, Gilberto S, Brito D, Moyer T, Kandels-Lewis S, *et al.* (2016). CDK1 prevents unscheduled PLK4-STIL complex assembly in centriole biogenesis. Curr Biol 26, 1127–1137.